

1 **Potential for Using a Tyre Pyrolysis Oil-Biodiesel Blend in a Diesel Engine**
2 **at Different Compression Ratios**

3 Abhishek Sharma* and S. Murugan

4 Internal Combustion Engines Laboratory

5 Department of Mechanical Engineering

6 National Institute of Technology Rourkela

7 Rourkela-769008 (India)

8 **Abstract**

9 This study is aimed at investigating effects of varying the compression ratio at optimum
10 injection timing and injection pressure on the behaviour of a diesel engine, using a non-
11 petroleum fuel, i.e. a blend of 80% biodiesel, and 20% oil obtained from pyrolysis of waste
12 tyres. The engine was subjected to one lower (16.5) and one higher (18.5) compression ratio
13 in addition to the standard compression ratio of 17.5. At the higher compression ratio of 18.5
14 and full load, shorter ignition delay, maximum cylinder pressure and higher heat release rate
15 were found for the blend, compared to those in case of the original compression ratio. The
16 increase in the compression ratio from 17.5 to 18.5 for the blend improved the brake thermal
17 efficiency by about 8% compared to that of the original compression ratio at full load. The
18 experimental results indicated that for the blend at a higher compression ratio of 18.5, the
19 brake specific carbon monoxide, brake specific hydrocarbon emissions and smoke opacity
20 were reduced by about 10.5%, 32%, and 17.4% respectively, with respect to those of the
21 original compression ratio at full load.

22
23 **Keywords:** Compression Ratio; Diesel Engine; Emission; Non Petroleum Fuel; Performance

24 *Corresponding author

25 Email ID: drasharma58@gmail.com

26 Phone: +91-9861897954

27 **1. Introduction**

28 As petroleum based fuels are found only in limited reserves in the world, it has become
29 imperative to explore alternative renewable fuels, which can be derived from other resources
30 that are easily available in the country. The other issue is that the combustion of fossil fuels is
31 the major source of global warming, ozone depletion and climate change and, it also has
32 detrimental effects on human health harmfully [1].

33
34 Diesel engines are widely used in several applications, because of their lean operation, high
35 thermal efficiency, lower fuel consumption and tendency to emit lower greenhouse gases
36 compared to the spark ignition (SI) engines. Different pollutants emitted from compression
37 ignition (CI) engines depend on many factors that include engine design parameters,
38 operational conditions, fuel type, and exhaust emission after treatment employed [2]. In order
39 to overcome these problems extensive research works were carried out in the last two
40 decades. Several researchers suggested that the use of biofuels in small quantities with the
41 conventional diesel fuel or as a sole fuel after a necessary fuel or engine modification would
42 certainly help to solve these problems [3-4]. Biodiesel, in particular has a significant potential
43 to be used as an alternative fuel for CI engines. It is the methyl or ethyl ester of fatty acids
44 made from edible or non-edible vegetable oils, animal fats and algae. Many countries use
45 different non-edible oils such as *Jatropha curcas*, *Pongamia pinnata*, *Madhuca indica*, Linseed
46 and edible oils such as palm, soybean, sunflower oil etc. [5-9] for biodiesel production. The
47 use of biodiesel in diesel engines results in significant reduction of unburned hydrocarbon
48 (HC), carbon monoxide (CO), smoke opacity and particulate matter. As there is no sulphur in
49 biodiesel, there is no or negligible oxides of sulphur emitted from the engine fueled with
50 biodiesel. It contains about 10% oxygen in the molecules, which improves the ignition
51 quality resulting in an enhanced combustion of the fuel inside the cylinder [10].

52 In spite of all these merits, the utilisation of biodiesel in CI engines is not proved to be a
53 promising alternative fuel in many countries, because it is produced in less quantity. There
54 are two possible options to solve this problem; one is replacing biodiesel by another non-
55 conventional fuel which is derived from organic wastes and the other one is to increase the
56 production rate. The former seems to be a better solution than the later, because it may reduce
57 the disposal and environmental problems.

58
59 Waste automobile tyre is an organic waste from which useful energy in the form of liquid,
60 gas or solid can be derived. Pyrolysis process, also termed as thermal distillation, is one of
61 the methods employed for obtaining such fuels. The energy rich liquid, gas and solid products
62 from pyrolysis of waste automobile tyres are referred to as viz., Tyre pyrolysis oil (TPO),
63 pyro gas, and carbon black respectively [11]. Among these, the TPO can be a potential
64 alternative fuel for CI engines but the main drawback is its lower cetane number, which is in
65 the range of 25-30. In a preliminary research work that was carried out in the past to study the
66 effect of Jatropha methyl ester (JME)-TPO blend on diesel engine behaviour, five different
67 blends (JMETPO10, JMETPO20, JMETPO30, JMETPO40 JMETPO50) were prepared. The
68 numeric value indicates the volume percentage of TPO in the blend. Experiments were
69 conducted in a constant speed, direct injection (DI) diesel engine, with a rated power of 4.4
70 kW at 1500 rpm. The test results confirmed that, the blend with 20% (by volume) TPO gave
71 a better performance and lower emissions than those given by other blends. Addition of 20%
72 TPO on to the blend resulted in substantial changes in the combustion, performance and
73 emission characteristics of the engine. It has been observed earlier that the combustion
74 commenced slightly later than in case of 100% biodiesel i.e. JME. However, it was found that
75 brake thermal efficiency (BTE) improved by about 4.5% while brake specific energy
76 consumption (BSEC) and brake specific nitric oxide emission (BSNO) reduced by about
77 1.9% and 7.9% respectively as compared to the case of using 100% JME [12].

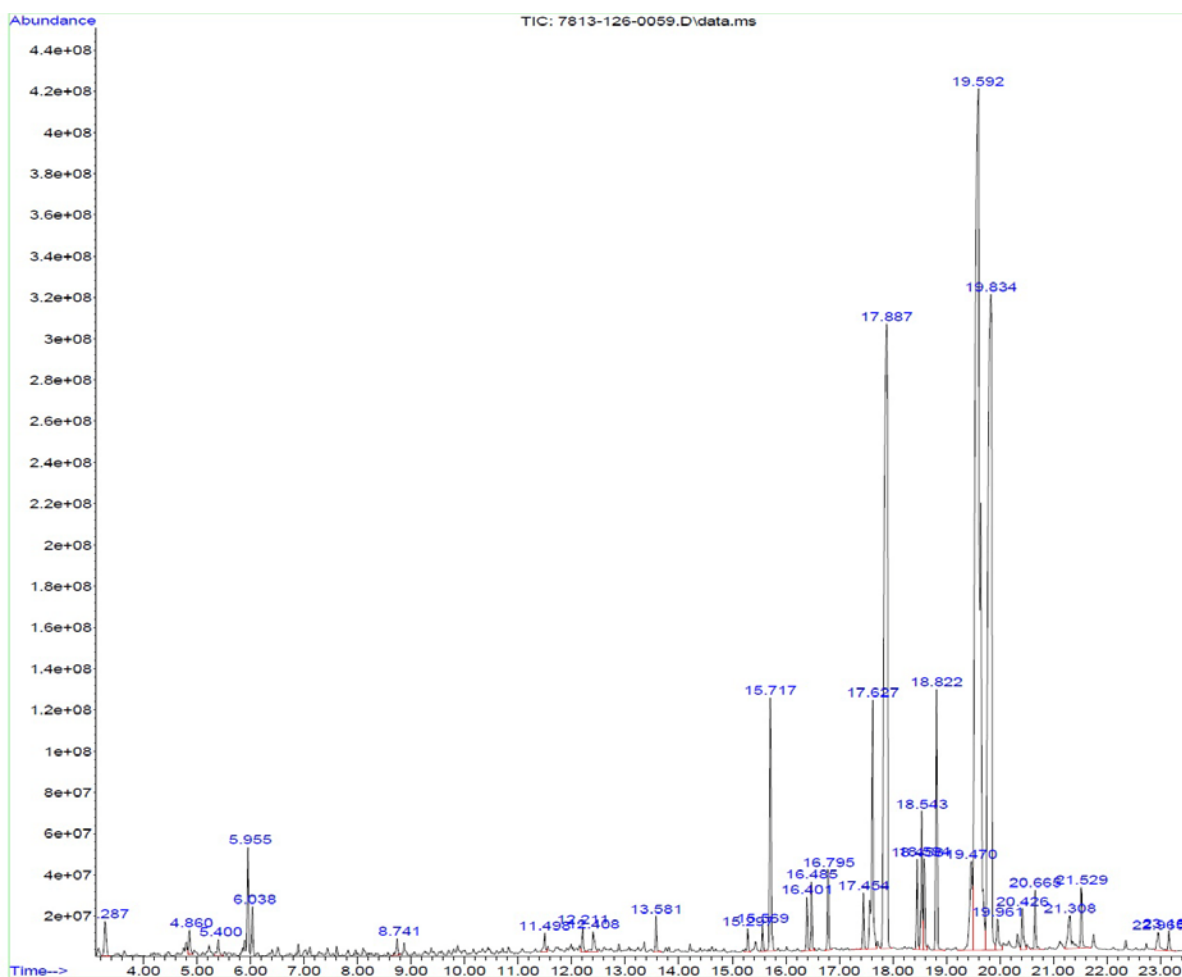
78 Several researchers have reported on the optimum design parameters for diesel engines when
79 fueled with alternative fuels, because the conventional diesel engine is designed only for
80 diesel fuel. Most of the investigations have documented the form of blends with different
81 alternative fuels, used in the existing diesel engine, or 100% biodiesel without any engine
82 modifications [13-15]. Also, experimental investigations were carried out to use higher
83 percentage of biodiesel by altering the engine, and to find the optimum engine design
84 parameters for a particular fuel [16-18]. Many researchers have reported results pertaining to
85 the effects of varying injection timing, nozzle opening pressure and compression ratio on
86 thermal efficiency, specific fuel consumption (SFC) and exhaust emissions of CI engines [19-
87 22]. It has been reported that the engine performance may be improved by many ways, such
88 as increasing the compression ratio, and nozzle opening pressure and advancing the fuel
89 injection timing. The use of a higher compression ratio usually enhances the fuel-air mixture
90 density, due to the increase in the pressure and temperature of the compressed mixture in the
91 combustion chamber, leading to a rise in peak cylinder pressure and the burning speed of the
92 fuel-air mixture. Experimental investigations were carried out in the past to evaluate the CI
93 engine characteristics at different compression ratios using various diesel-biodiesel blends
94 [23-25].

95
96 Experiments were carried out on a diesel engine using JMETPO20 (containing 80% JME +
97 20% TPO in volume basis) blend at varied injection timings and nozzle opening pressures. It
98 was found by the authors that an advanced injection timing of 24.5 °CA bTDC and higher
99 nozzle opening pressure of 220 bar improved the overall performance of the engine [26-27].

100 This experimental investigation was aimed to study the effects of operating the engine fueled
101 with the JMETPO20 at different compression ratios, one higher (18.5) and one lower (16.5)
102 in addition to the original compression ratio of 17.5 keeping the injection timing and nozzle
103 opening pressure of the engine at optimum conditions.

104 **2. Materials and methods**

105 The TPO was blended with the JME on a 20/80% volume basis and the blend was kept under
106 observation for 30 days, to ensure its stability. The details of preparation of JME and TPO
107 have been described by the authors in elsewhere [12]. It was noticed that the TPO was not
108 separated from the JME in the blend. Gas chromatography/Mass spectrometer (GC/MS) was
109 used for analysing the composition of the blend, as shown in Fig.1. The GC-MS of the blend
110 indicates that it contains compounds, like Pentadecanoic acid methyl ester, 10-Octadecenoic
111 acid methyl ester, and Heptadecanoic acid methyl ester in large proportions. All the
112 functional groups show the existence of oxygen, which is due to the presence of JME in the
113 blend. Table 1 gives the comparison of the physico chemical properties of diesel, JME, TPO
114 and the JMETPO20 blend.



115

116

Fig. 1 GC-MS chromatogram of the JMETPO20 blend

117 **Table 1 Physico-chemical properties of diesel, JME, TPO and the JMETPO20 blend**

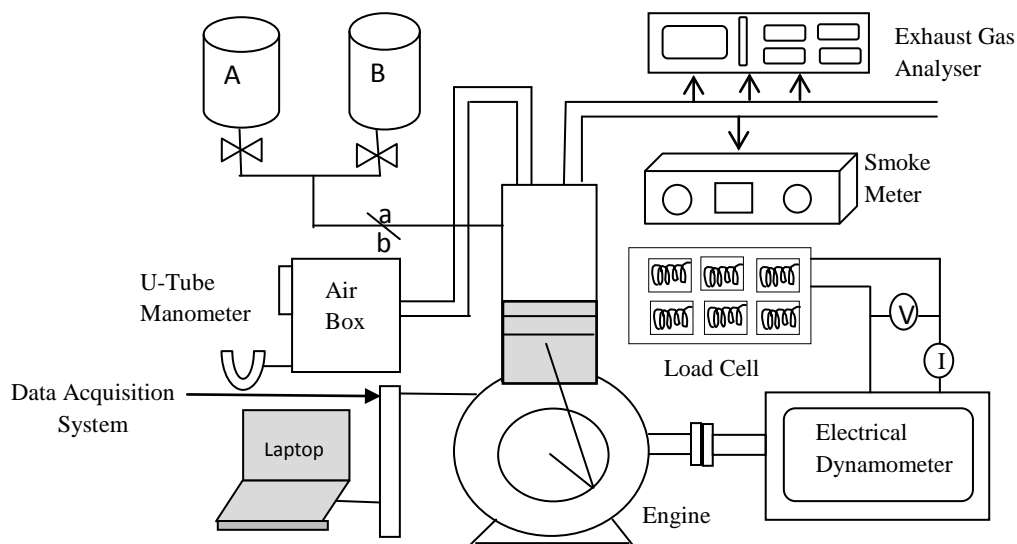
Properties	ASTM Test Method	Diesel	JME	TPO	JMETPO20
Specific gravity	D 4052	0.830	0.881	0.913	0.887
Viscosity (cSt)	D 445	2.6	5.6	3.35	5.2
Calorific Value	D 4809	43.8	39.4	38.1	38.82
Flash point (°C)	D 93	50	156	49	132
Fire point (°C)	D 93	56	171	58	145
Cetane number	D 613	50	55	28	52
Carbon (%)	D 3178	86.2	77.1	86.92	79.26
Hydrogen (%)	D 3178	13.2	11.81	10.46	11.31
Nitrogen (%)	D 3179	Nil	0.119	0.65	0.23
Sulphur (%)	D 3177	0.3	0.001	0.95	0.18
Oxygen by	E 385	Nil	10.97	1.02	9.02

118

119 **3 Test details**

120 The investigation was carried out on a naturally aspirated, DI diesel engine, with a rated
 121 power of 4.4 kW at 1500 rpm. The technical specifications of the engine are listed in Table 2.
 122 Figure 2 shows the schematic layout of the engine experimental set up used in the
 123 investigation. The engine was coupled with an eddy current dynamometer for loading. The
 124 air consumption was measured using a sharp-edged orifice plate and U-tube manometer. A
 125 burette fitted with two optical sensors, one at a high level and, the other at a low level, was
 126 employed for measuring the fuel flow to the engine. The liquid flow through the high level
 127 optical sensor, gives a signal to the computer to start the time. Once the fuel reached the
 128 lower level optical sensor, the sensor would give the signal to the computer, to stop the time
 129 and refill the burette. The time taken for the consumption of fuel of a fixed volume was
 130 recorded. The engine exhaust gas temperature was measured using a K type (Chromel-

131 Aluminium) thermocouple connected to a digital indicator. The Kistler type piezoelectric
 132 pressure transducer was mounted on the cylinder head for the measurement of the cylinder
 133 pressure. A top dead centre (TDC) encoder was used to detect the engine crank angle. The
 134 engine setup was attached with a control panel, which had the capability to communicate
 135 with the pressure sensor, and to convert the signal from the pressure sensor to the analogue
 136 voltage signal, which was fed to the data acquisition system (DAS). The exhaust gas
 137 compounds such as CO, CO₂, HC, NO, and O₂ were measured with the help of an AVL
 138 DiGas 444 exhaust gas analyser. The smoke opacity of the exhaust gas was measured by an
 139 AVL 437 diesel smoke meter.



148 **Fig. 2 Schematic layout of the experimental setup**

149 The measurements of various parameters were recorded only after the engine attained the
 150 steady state. Each test was conducted for 3 times, ensuring the repeatability of the result. The
 151 values given in this study are the averages of these results. During the tests, the engine ran
 152 satisfactorily through the entire duration, and did not show any difficulty, when fueled with
 153 the JMETPO20 blend. Initially, the experiments were conducted using diesel and the
 154 JMETPO20 blend, under the original injection timing of 23° CA bTDC, nozzle opening

155 pressure of 200 bar and compression ratio of 17.5, as set by the engine manufacturer for
156 obtaining the reference data.

157 Table 2 Technical specifications of the test engine

Manufacturer	Kirloskar
Model	TAF 1
Engine type	Single cylinder, four stroke, constant speed, air cooled, direct injection, CI engine
Rated power (kW)	4.4
Speed (rpm)	1500 (constant)
Bore (mm)	87.5
Stroke (mm)	110
Piston type	Bowl-in-piston
Displacement volume (cm ³)	661
Compression ratio	17.5
Nozzle opening pressure (bar)	200
Start of fuel injection	23 °CA bTDC
Dynamometer	Eddy current
Injection type	3- Hole pump-line-nozzle injection system
Nozzle type	Multi hole
No. of holes	3

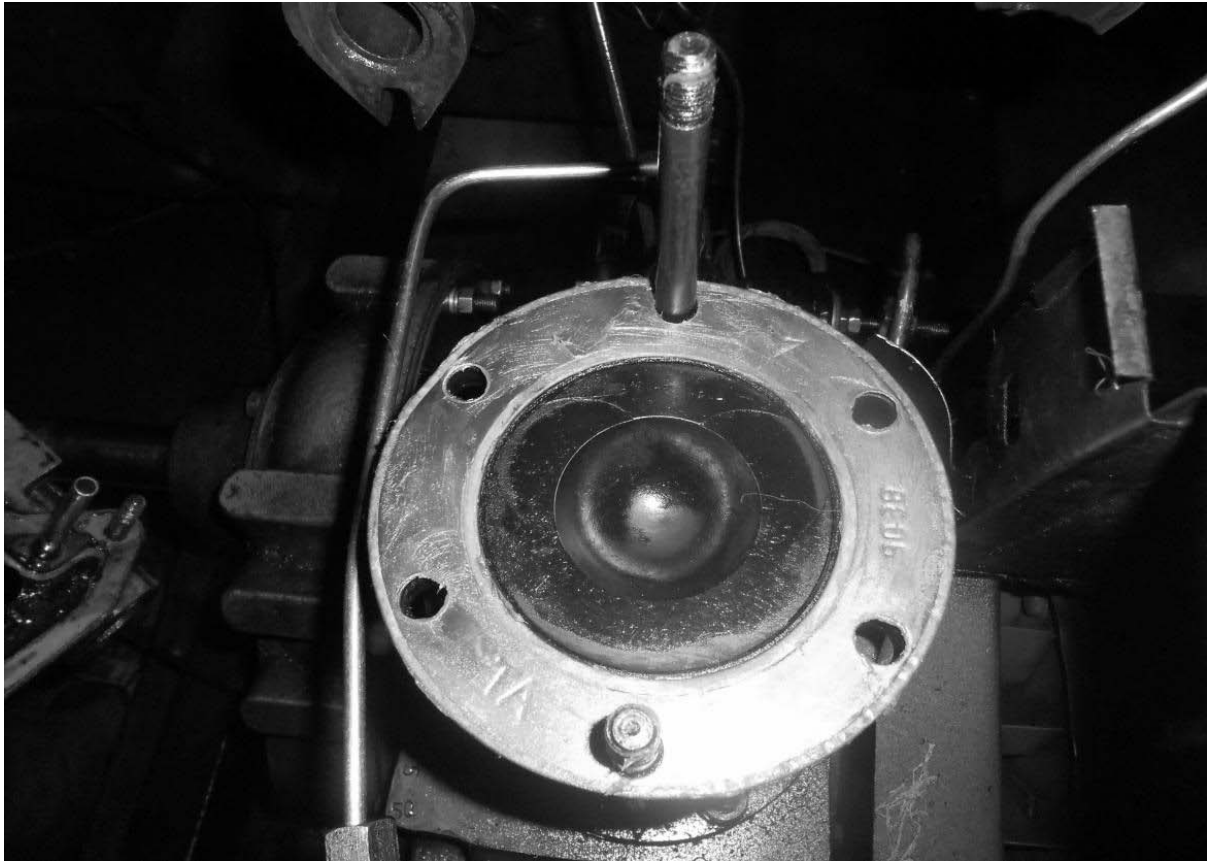
158
159 Further, the experiments were conducted with the advanced injection timing of 24.5°CA and
160 injection pressure of 220 bar, using the JMETPO20 blend for the compression ratios of 16.5,
161 17.5 and 18.5. The compression ratio of the engine was altered by changing the clearance
162 volume, by the replacement of gaskets of different thickness in between the cylinder and the
163 cylinder head. Fig.3 shows the photographic view of the gasket fitted with cylinder block.
164 The compression ratio below 16.5 resulted in a poor performance, and a compression ratio
165 above 18.5 was not attainable, owing to the engine structural constraint.

166 The steps involved in the calculation of the compression ratio are as follows:

167 Compression Ratio (CR) = $\frac{\text{Maximum cylinder volume (Vs+ Vc)}}{\text{Clearance volume (Vc)}}$

168 Maximum cylinder volume = Swept volume (Vs) + Clearance volume (Vc)

169



170

171

Fig. 3 Standard gasket fitted with cylinder block

172

$$V_s = \frac{\pi d^2}{4} \times L \quad (\text{Where, } d = \text{bore} = 8.75 \text{ cm, } L = \text{Stroke} = 11 \text{ cm})$$

173

$$CR = 17.5 = \frac{V_s + V_c}{V_c}$$

174

$$17.5 = \frac{V_s}{V_c} + 1$$

175

$$16.5 = \frac{V_s}{V_c}$$

176

$$V_c = \frac{V_s}{16.5} = \frac{661.45}{16.5} = 40.08 \text{ cm}^3$$

177

Gasket volume = 7.21 cm^3 ($d = 8.75 \text{ cm, } t = 0.12 \text{ cm}$)

178

For $CR = 18.5$, $V_c = \frac{V_s}{17.5} = \frac{661.45}{17.5} = 37.79 \text{ cm}^3$

Clearance Volume excluding gasket volume+ Gasket volume = 37.79 cm³

32.87 + Gasket volume = 37.79 cm³

Gasket volume required for compression ratio of 18.5 = 4.92 cm³

Gasket thickness required = 0.08 cm

In the same manner, the gasket volume and thickness required for CR=16.5 was calculated.

The calculated gasket volume and thickness corresponding to the different compression ratios

are given below in Table 3.

Table 3 Gasket volume and thickness required for different compression ratios

Compression ratio	Gasket volume (cm ³)	Gasket thickness (cm)
16.5	9.8	0.16
17.5	7.21	0.12
18.5	4.92	0.08

4. Results and discussion

Compression ratio is known to have substantial impact on the behaviour of a CI engine.

Therefore, the effects of the compression ratio on the combustion, performance and exhaust

emissions of a single cylinder CI engine fueled with the JMETPO20 blend investigated

experimentally and the test results are presented in the subsequent sections. The experiments

were conducted at the advanced injection timing of 24.5°CA and higher injection pressure of

220 bar, for the compression ratios of 16.5, 17.5 and 18.5, and the results are compared with

those of diesel operation under standard test conditions.

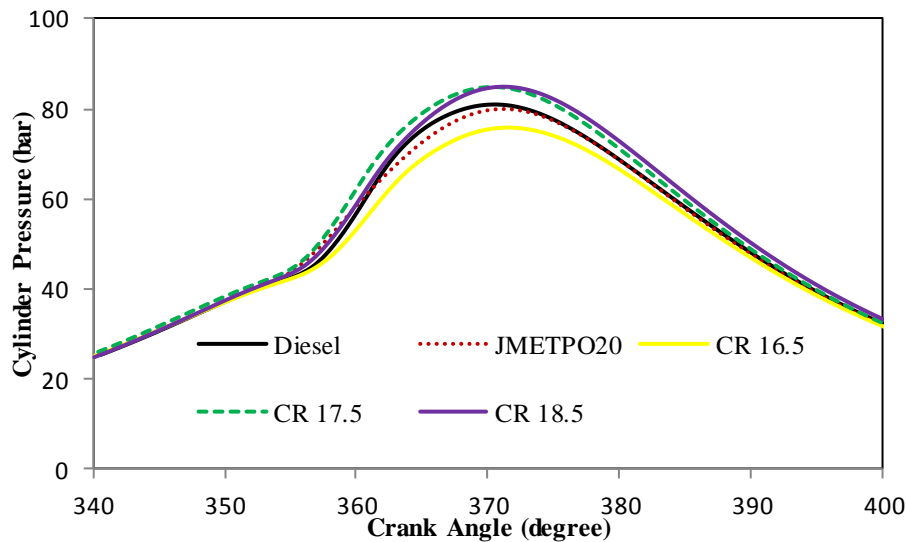
4.1 Combustion analysis

The cylinder pressure crank angle diagram is employed to analyse the engine combustion

behaviour, as the cylinder pressure has an effect on the performance parameters and emission

levels of the engine. The variations of the cylinder pressure with respect to the crank angle

198 (CA) at different compression ratio, for diesel and the blend at full load are shown in Fig.4.
199 The peak pressure in a CI engine depends primarily on the combustion rate in the initial
200 stages, and is influenced by the fuel taking part in the premixed combustion phase [28].



201

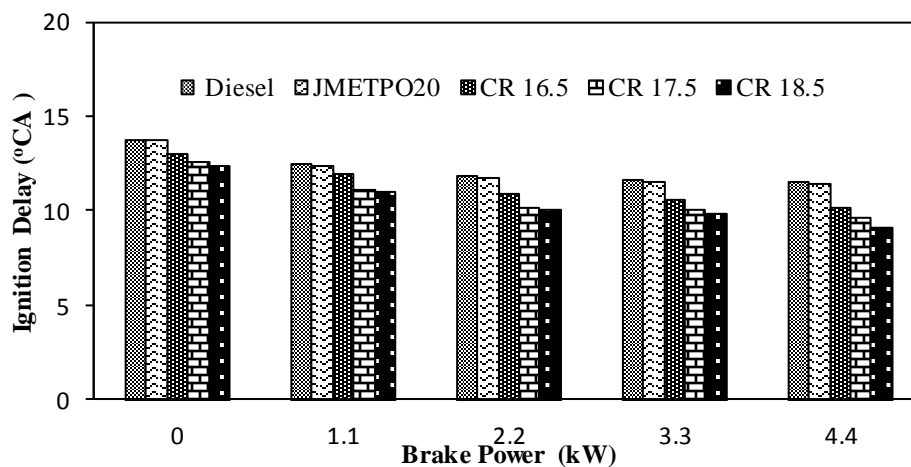
202 Fig.4 Cylinder pressure versus CA at different compression ratios

203 The cylinder pressures for diesel and the blend are obtained as 80.9 bar at 370.30 °CA and
204 79.9 bar at 371 °CA respectively, at the original compression ratio and full load. It is found
205 that the combustion starts slightly earlier for the blend than for diesel at the original
206 compression ratio. This is because of the higher cetane number and presence of oxygen in the
207 blend, which results in improved combustion. The values of the maximum cylinder pressure
208 for the blend at full load have been recorded as 75.8 bar at 371.7 °CA, 84.9 bar at 370.4 °CA
209 and 85 bar at 371.4 °CA at compression ratios of 16.5, 17.5 and 18.5, respectively. It can be
210 observed from the figure, that from a lower to a higher compression ratio, the maximum
211 cylinder pressure is increased for the blend. The reason is that with the increase in the
212 compression ratio, the intake air temperature increases, which provides better fuel
213 atomization and mixture preparation with the air, and accelerates the complete combustion
214 process [29]. The maximum cylinder pressure for the blend is found to be enhanced by about
215 6.2% at the compression ratio of 18.5 and full load, compared to that of the original

216 compression ratio. For the blend at the lower compression ratio of 16.5, the maximum
 217 cylinder pressure is found to be lower compared to the original and the higher compression
 218 ratio, because of the relatively slower premixed combustion phase that ends up in a lower
 219 maximum cylinder pressure.

220
 221 **4.1.2 Ignition delay**

222 Ignition delay (ID) is a period measured in terms of CA between the beginning of fuel
 223 injection and the beginning of combustion [30]. The ID depends on parameters, such as the
 224 fuel quality, atomization of fuel and duration of injection, air-fuel ratio, engine speed,
 225 cylinder gas pressure, intake-air temperature, injection pressure, and compression ratio [31].
 226 Fig.5 compares the ignition delays of diesel and the blend with respect to brake power at
 227 three different compression ratios. As shown in the figure, as the load increases, the ID
 228 decreases for both the fuels at all compression ratios. This is because, as the engine load
 229 increases, the heat loss during compression decreases, resulting in higher temperature and
 230 pressure of the compressed air, and a shorter ID is obtained [32]. At the original compression
 231 ratio and full load, the values of the ID for diesel and the blend are about 11.5 and 11.4 °CA
 232 respectively. For the blend at full load, the values of ID are 10.1, 9.6 and 9.1 °CA at the
 233 compression ratios of 16.5, 17.5 and 18.5 respectively.



234

235 **Fig.5 Ignition delay versus brake power at different compression ratios**

236 The lowest value of ID is recorded as 9.1 °CA, at the compression ratio of 18.5 and full load
 237 for the blend and, it is found to be shorter by about 2.3 °CA, compared to the values at the
 238 original compression ratio. The increase in the compression ratio increases the compressed
 239 air temperature, which reduces the viscosity of the blend, by breaking down the
 240 intermolecular bonds, and decreasing the self ignition temperature of the fuel; and hence, the
 241 ID is shorter [33].

242
 243 **4.1.3 Heat release rate**

244 The comparison of the heat release rate (HRR) curve at full load for diesel and the blend at
 245 different compression ratios is depicted in Fig.6. The HRR is an important parameter for the
 246 analysis of the combustion phenomenon in the engine cylinder, as the combustion duration
 247 and ignition delay can be easily estimated from the HRR-CA diagram. The HRR in this study
 248 was calculated, by using the cylinder pressure data [34]. The HRR at each °CA was
 249 determined by the following formula, which is governed by the first law of thermodynamics.

250
$$\frac{dQ}{d\theta} = P \frac{\gamma}{\gamma-1} \left(\frac{dV}{d\theta} \right) + \frac{1}{\gamma-1} V \frac{dP}{d\theta} \dots\dots\dots \text{Eq}^n1$$

251 where dQ/dθ is the HRR (kJ/deg), P is the incylinder gas pressure (bar), V is incylinder
 252 volume (m³), and γ is the ratio of specific heats.

253 Figure 7 indicates that, the value of the HRR is the maximum for diesel, compared to that of
 254 the blend at all compression ratios. This may be attributed to the higher calorific value of
 255 diesel; and more fuel accumulating owing to longer ID would increase the amount of fuel
 256 burnt during the premixed combustion phase, causing a higher HRR. At full load, the values
 257 of the HRR for diesel and the blend are found to be about 56.4 and 50.4 J/°CA respectively,
 258 at the original compression ratio. At full load, the values of the maximum HRR in case of the
 259 blend are 42.3, 54.5 and 55.6 J/CA, for the compression ratios of 16.5, 17.5 and 18.5
 260 respectively.

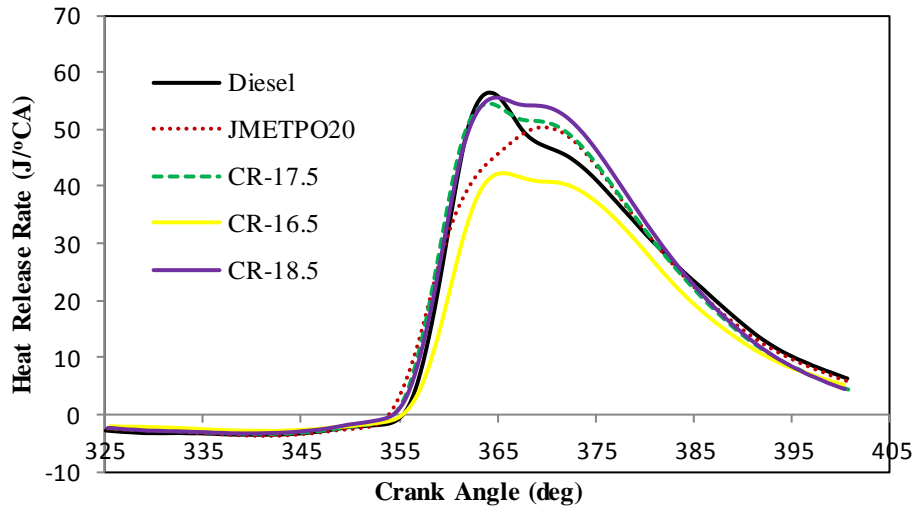
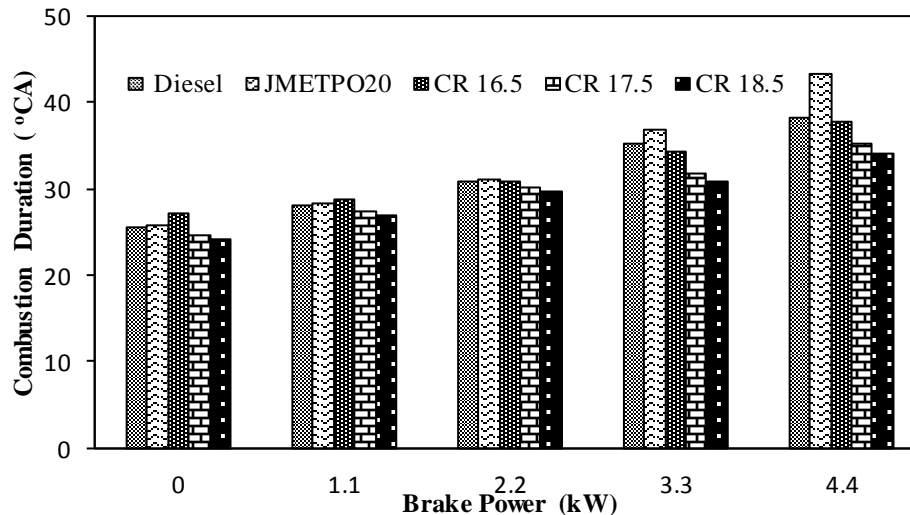


Fig.6 Heat release rate versus CA at different compression ratios

The HRR of 55.6 J/°CA is obtained for the blend at the compression ratio of 18.5, which is 10.3% higher than that of the original compression ratio at full load. The higher compression ratio enhanced the HRR for the blend due to the reduction in viscosity, and this might promote a better spray formation as the intake air temperature increases with a higher compression ratio [35]. The lower HRR is observed for the blend at a lower compression ratio of 16.5, due to the slower air-fuel mixture formation, weak air entrainment and poorer combustion of the fuel.

4.1.4 Combustion duration

The combustion duration (CD) is described as the time duration required by the combustion process to reach 90% of its mass fractions burned [36]. Fig. 7 depicts the variation of the CD for diesel and the blend at different compression ratios. The CD becomes longer with the increase in the engine load for both the fuels, owing to the increase in the quantity of fuel injected. At the original compression ratio and full load, the values of the CD for diesel and the blend are found to be about 38.3 and 43.3 °CA respectively.



278

279 **Fig. 7 Combustion duration versus brake power at different compression ratios**

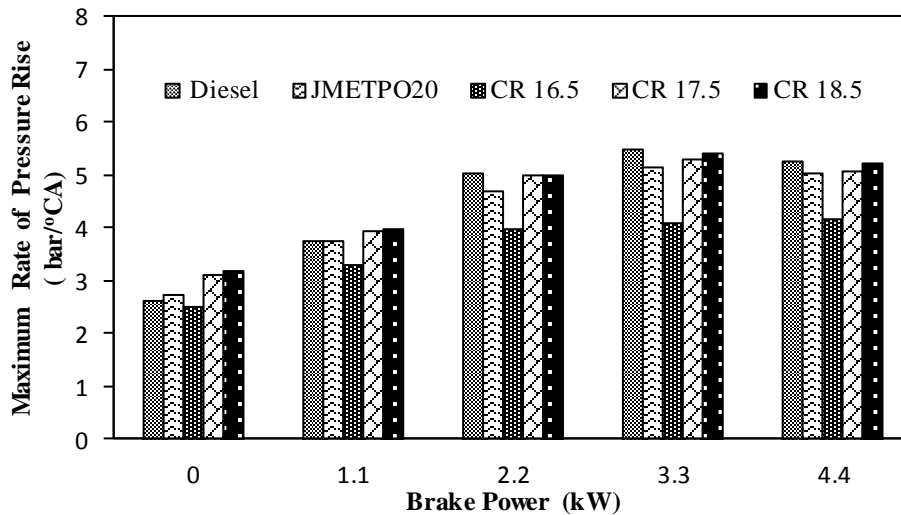
280 The longer CD obtained with the blend, at the original compression ratio is the result of an
 281 increase in the quantity of fuel consumed, to maintain the engine speed stable at different
 282 loads, as the calorific value of the blend is lower than that of diesel. The values of the CD are
 283 found to be about 37.9, 35.4 and 34.2 °CA, at the compression ratios of 16.5, 17.5 and 18.5
 284 respectively, at full load. The lowest value of CD of 34.2 °CA is observed with the
 285 compression ratio of 18.5 for the blend, at full load. The increase in CD causes a rise in the
 286 in-cylinder air temperature and pressure that provides faster fuel vaporization, and accelerates
 287 the complete combustion process and a decrease in the CD [37].

288

289 **4.1.5 Maximum rate of pressure rise**

290 The variation of the maximum rate of pressure rise (MRPR) with brake power for diesel and
 291 the blend at different compression ratios, is shown in Fig.8. The MRPR $(dp/d\theta)_{max}$ in an
 292 engine combustion chamber has a substantial impact on the maximum cylinder pressure and
 293 smoothness of the engine operation. In general, it is considered that combustion is normal
 294 when $(dp/d\theta)_{max}$ is lower than 3 bar/ °CA whereas the engine is considered to be knocking, if
 295 is greater than 7 to 8 bar/ °CA [38]. The MRPR at the original compression ratio for diesel
 296 varies from 2.6 bar/°CA at no load to 5.3 bar/°CA at full load, and for the blend it varies from

297 2.7 bar/°CA at no load to 5 bar/°CA at full load. The MRPR is found to be rising with
 298 increase in compression ratio for the blend from no load to full load. The MRPR at full load
 299 is found to be the highest as 5.2 bar/°CA for the blend at compression ratio of 18.5.



300

301 **Fig. 8 Maximum rate of pressure rise versus brake power at different compression**
 302 **ratios**

303 The oxygen enrichment in the blend due to the addition of JME accelerates the reactions, and
 304 this result in more complete combustion of fuels which is the cause for the increase in the
 305 maximum rate of pressure rise at a higher compression ratio [39]. The values of the MRPR at
 306 compression ratios of 16.5, 17.5 and 18.5, are found to be about 4.2, 5.1 and 5.2 bar/°CA
 307 respectively, for the blend at full load.

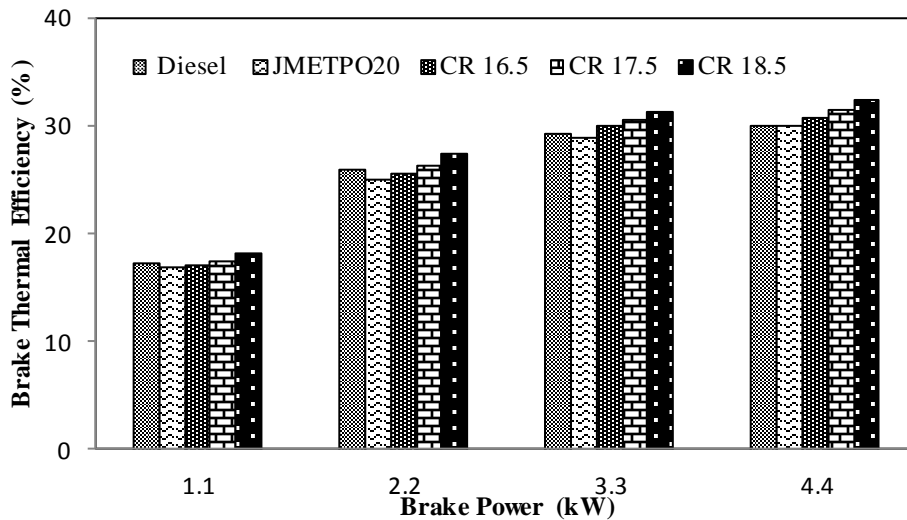
308

309 **4.2 Performance analysis**

310 **4.2.1 Brake thermal efficiency**

311 Figure 9 shows the effect of the compression ratios on the brake BTE for diesel and the
 312 blend. The BTE is given by the ratio between the power output and the product of the fuel
 313 mass flow rate and lower heating value of the fuel [40]. It is clear from the figure, that the
 314 BTE is found to increase considerably with an increase in the load as a reduction in the heat
 315 loss and increase in power are encountered at higher loads. The values of BTE for diesel and

316 the blend are very close to each other. The results indicate that the BTE of diesel and the
 317 blend at full load were acquired as 29.9% and 29.8% respectively at the original compression
 318 ratio. Generally, increasing the compression ratio improved the BTE of the engine. This is
 319 due to the fact that at a higher compression ratio, the compressed air temperature is higher,
 320 which ends up in better combustion of the fuel.



321

322 **Fig. 9 Brake thermal efficiency versus brake power at different compression ratios**

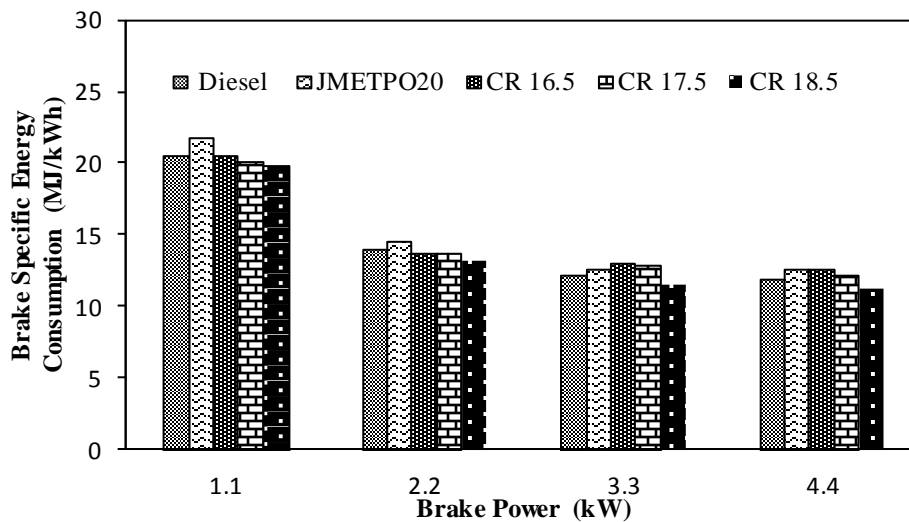
323 The BTE for the blend at full load was obtained as 30.7%, 31.4% and 32.3% at compression
 324 ratios of 16.5, 17.5 and 18.5, respectively. The blend has the highest BTE with 32.3% at the
 325 compression ratio of 18.5, and it is about 8% higher than that of diesel. The possible reason
 326 for this may be the proper mixing of the fuel-air, and improved fuel spray characteristics that
 327 occurred with the higher compression ratio of 18.5. At full load, the BTE for the blend at the
 328 compression ratio of 16.5 was decreased by about 2.2% and 4.8% compared to that of the
 329 compression ratios of 17.5 and 18.5, respectively. The mechanical efficiency of diesel and the
 330 blend were acquired as 84% and 83.2% respectively at the original compression ratio and full
 331 load. The values of mechanical efficiency for the blend were about 83.4%, 84% and 85% at
 332 compression ratios of 16.5, 17.5 and 18.5 and full load, respectively.

333

334

335 **4.2.2 Brake specific energy consumption**

336 The brake specific fuel consumption (BSFC) is not always a reliable factor when two fuels of
337 different calorific values and densities are blended together [41]. The BSEC is described as
338 the multiplication of the BSFC and lower calorific value of the fuel.



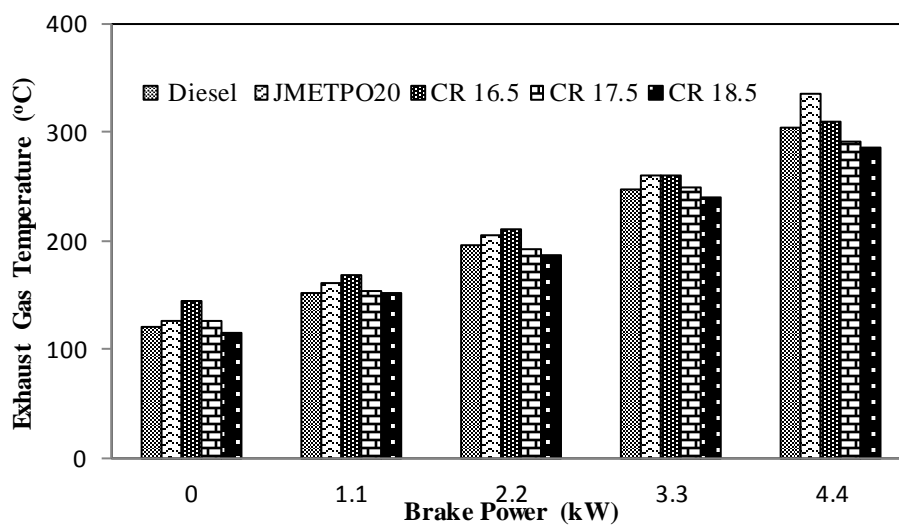
339

340 **Fig. 10 Brake specific energy consumption versus brake power at different compression**
341 **ratios**

342 Fig. 10 illustrates the variation of the BSEC for diesel and the blend with the brake power at
343 different compression ratios. At the original compression ratio and full load, the values of
344 BSEC for diesel and the blend were recorded as 11.9 and 12.6 MJ/kWh respectively. The
345 BSEC for the blend at full load was obtained as 12.5, 12.1 and 11.2 MJ/kWh at compression
346 ratios of 16.5, 17.5 and 18.5, respectively. From the figure it is clear that while increasing the
347 compression ratio of the engine the BSEC will be reduced for the blend. The lowest value of
348 BSEC for the blend is found to be about 11.2 MJ/kWh, at full load and original compression
349 ratio. The possible reason may be that higher compression ratio enhances the extent of
350 evaporation and subsequently the combustion process. But, with the lower compression ratio,
351 the BSEC is increased owing to incomplete combustion, resulting in a lowered power output
352 and decreased BTE.

353 **4.2.3 Exhaust gas temperature**

354 The analysis of the exhaust gas temperature (EGT) gives qualitative information on the
355 combustion of the fuel [42]. The variations of the EGT for different compression ratios are
356 shown in Fig. 11. With the increase in engine load, the EGT is found to increase due to
357 higher combustion temperature inside the cylinder as more fuel is burnt with increasing load.
358 At the original compression ratio, the values of EGT are found to be about 303 and 335 °C
359 for diesel, and the blend respectively, at full load. For the blend as the compression ratio
360 increases, the EGT decreases. At full load the values of EGT for the blend are recorded as
361 310, 290 and 285 °C for the compression ratios of 16.5, 17.5 and 18.5 respectively. The blend
362 has the lowest value of EGT at compression ratio of 18.5 and it is lower by about 18 °C as
363 compared to that for diesel at full load.



364

365 **Fig. 11 Exhaust gas temperature versus brake power at different compression ratios**

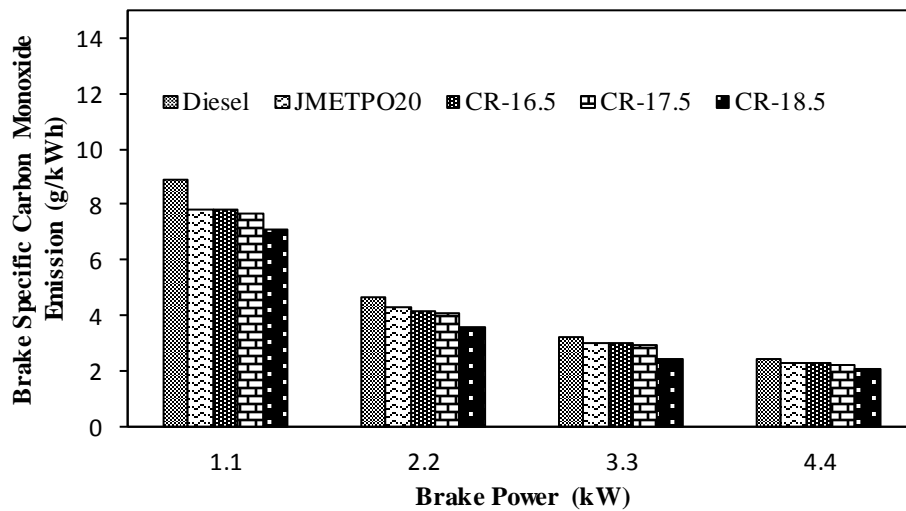
366 This may be due to the fact that air entered during the suction stroke at higher compression
367 ratio is compressed, which increases the air temperature. The increased air temperature helps
368 for better atomization of fuel which contributes in complete combustion and resulting
369 reduction in the EGT. At lower compression ratio of 16.5 the EGT for the blend is higher as

370 to more amount of heat is released during diffusion phase resulting in more amount of heat
371 going along with exhaust gas.

372
373 **4.3 Emission analysis**

374 **4.3.1 Brake specific carbon monoxide emission**

375 It is known that the rate of CO emission is a function of the unburned fuel availability and
376 mixture temperature, which controls the rate of fuel decomposition and oxidation. In the
377 presence of sufficient oxygen, the CO emission is converted into CO₂ [43].



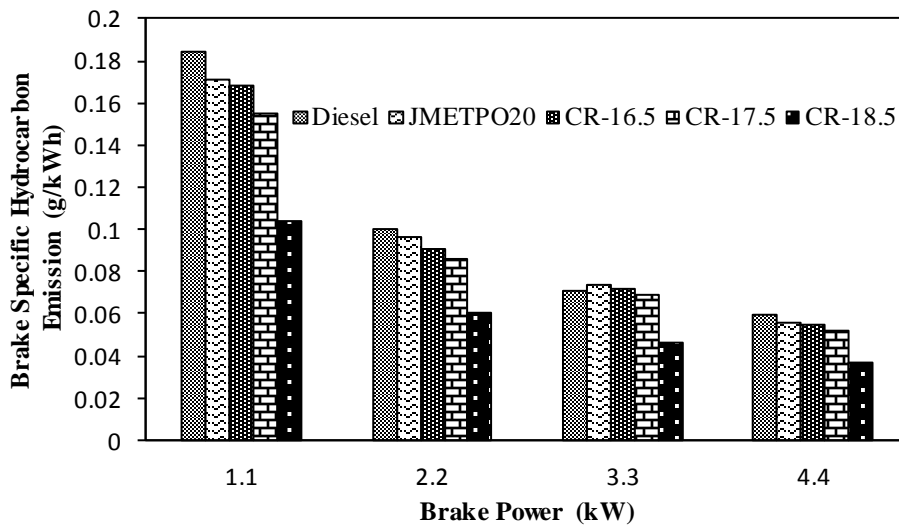
378
379 Fig. 12 Brake specific carbon monoxide emission versus brake power at different
380 compression ratios

381 The brake specific carbon monoxide (BSCO) emission results are illustrated in Fig.12 at
382 different compression ratios of the blend, in comparison to those for diesel. The BSCO
383 emissions for diesel and for the blend at the original compression ratio and full load are about
384 2.5 and 2.3 g/kWh respectively. The BSCO for the blend at full load was obtained as 2.3, 2.2
385 and 2 g/kWh at compression ratios of 16.5, 17.5 and 18.5, respectively. The BSCO emission
386 for the blend is marginally lower on increasing the compression ratio to 18.5, compared to the
387 original compression ratio. This could be due to the fact that that the increased compression
388 ratio increases the air temperature inside the cylinder subsequently reducing the delay period

389 leading to better and more complete burning of the fuel and so lower BSCO emission [44].
 390 The lower value of BSCO emission at full load for the blend was found to be 2 g/kWh, at the
 391 compression ratio of 18.5.

392
 393 **4.3.2 Brake specific hydrocarbon emission**

394 The HC emission consists of fuel that is completely unburned or alone partially burned. The
 395 HC emission is influenced by the fuel-air mixing, and is abundantly affected by the overall
 396 air-fuel equivalence ratio, as the equivalence ratio varies broadly from very rich at the core of
 397 the spray to very lean at the spray boundaries [45]. The brake specific hydrocarbon (BSHC)
 398 emission results at different compression ratios for diesel and the blend are illustrated in
 399 Fig.13. The BSHC emissions for diesel and the blend at the original compression ratio are
 400 about 0.059 and 0.055 g/kWh respectively at full load.



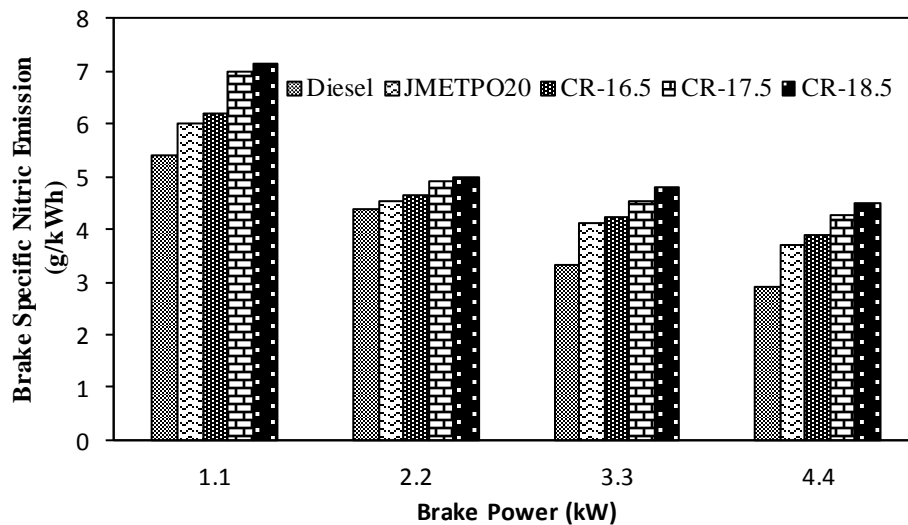
401
 402 **Fig. 13 Brake specific hydrocarbon emission versus brake power at different**
 403 **compression ratios**

404 The figure shows that the BSHC emission of the blend, is lower at the higher compression
 405 ratio of 18.5. At the compression ratio of 18.5, the minimum BSHC emission of about 0.037
 406 g/kWh is obtained with the blend, which is lower by about 32%, compared to the original
 407 compression ratio at full load. The increase in compression ratio enhances the air density and

408 temperature in the cylinder, resulting in better fuel-air mixing in the combustion chamber,
 409 which contributes to the more complete combustion of the fuel. The BSHC emission for the
 410 blend was measured to be 0.055, 0.052, and 0.037 g/kWh, at the compression ratios of 16.5,
 411 17.5 and 18.5, respectively and full load.

412
 413 **4.3.3 Brake specific nitric oxide emission**

414 The formation of nitric oxide (NO) emission is highly dependent on the maximum
 415 temperature of burned gases during the premixed combustion phase, oxygen concentration,
 416 and the time available for the reactions to take place [46]. Fig.14 presents the BSNO emission
 417 values for diesel and the blend at different compression ratios. The BSNO emissions for the
 418 blend at full load are found to be about 3.9, 4.3, and 4.5 g/kWh, at the compression ratios of
 419 16.5, 17.5 and 18.5, respectively.



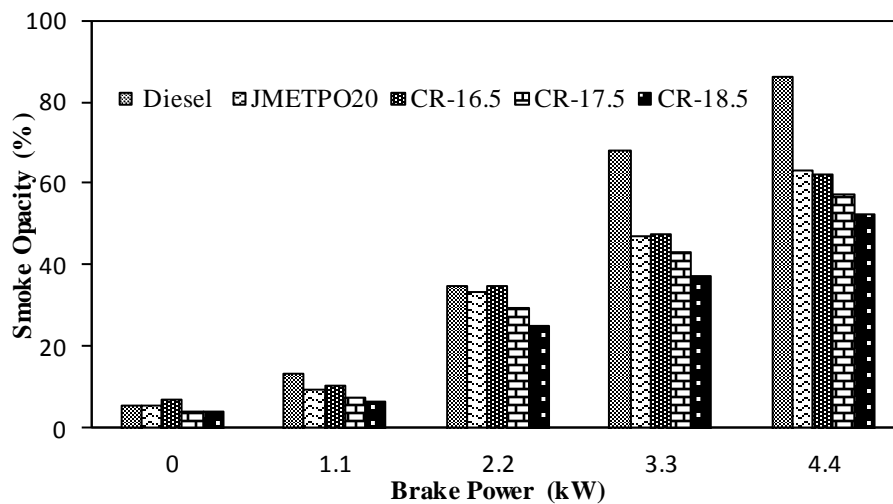
420
 421 **Fig. 14 Brake specific nitric oxide emission versus brake power at different compression**
 422 **ratios**

423 As observed in this figure, for the blend, at the higher compression ratio of 18.5, the BSNO
 424 emission is boosted compared to the original and lower compression ratio. It is quite obvious
 425 that at the higher compression ratio, the temperature in the combustion chamber is expected
 426 to be higher due to improved combustion, and also the amount of oxygen present in the

427 blend, results in higher amount of NO formation. The increase in the air intake temperature
 428 due to the rise in the compression ratio generates faster combustion rates, resulting in higher
 429 burned gas temperatures. The BSNO emission is decreased for the blend, while decreasing
 430 the compression ratio to 16.5, compared to that of the original compression ratio, because of
 431 lower premixed heat release rates, which cause a lower combustion temperature. In India, as
 432 per emission norms of central pollution control board, the acceptable range for BSCO, BSHC
 433 and BSNO emissions is 3.5, 1.3 and 9 g/kWh respectively for stationary diesel engine.

434
 435 **4.3.4 Smoke opacity**

436 The smoke formation depends mainly on the incomplete burning of the hydrocarbon fuel, and
 437 partially reacted carbon content in the liquid fuel [47]. The results of smoke opacity are
 438 depicted in Fig.15 at different compression ratios. It is apparent from the figure that the
 439 smoke opacity grows with rise in the engine load due to the overall richer combustion, longer
 440 duration of the diffusion phase and reduced oxygen concentration [48].



441
 442 **Fig. 15 Smoke opacity versus brake power at different compression ratios**

443 At the original compression ratio, the smoke opacity for diesel and the blend is about 86.3%
 444 and 63.1% respectively, at full load. At the original compression ratio for the blend, the
 445 smoke opacity is relatively less in comparison with diesel, due to the presence of oxygen in

446 the blend that contributes to a complete fuel oxidation. This actually leads to a significant
447 drop in smoke opacity. For the blend at the compression ratio of 18.5, the smoke opacity is
448 lower by about 17.4%, compared to that of the original compression ratio at full load. At full
449 load, the values of smoke opacity for the blend are about 62.3%, 57.1%, and 52.1%, at the
450 compression ratios of 16.5, 17.5 and 18.5, respectively. The smoke opacity reduced at the
451 higher compression ratio of 18.5 compared to the original and lower compression ratio,
452 because as the compression ratio increases, the combustion temperature increases due to
453 improved fuel atomization, and this leads to the reduction in smoke opacity.

454 **5. Conclusions**

456 Experimental investigations were carried out to study the behaviour of a single cylinder, four
457 stroke, air cooled, constant speed, DI diesel engine running on JMETPO20 blend, at varying
458 compression ratio from 16.5 to 18.5, has been made. The conclusions of the experimental
459 investigation are as follows:

- 460 • The maximum cylinder pressure and heat release rate at the compression ratio of 18.5
461 were higher by about 6.2% and 10.3% respectively, than those of the original
462 compression ratio.
- 463 • The ignition delay period decreased by about 2.25 °CA at the compression ratio of
464 18.5 than that of the original compression ratio.
- 465 • It is found that increasing the compression ratio of the engine, the brake thermal
466 efficiency is enhanced irrespective of the engine load. The maximum brake thermal
467 efficiency obtained at the compression ratio of 18.5 is higher by about 8% than that of
468 the original compression ratio. Also it was found that at the compression ratio of 18.5
469 the BSEC of the engine running with the blend was reduced by about 11% compared
470 to original compression ratio.

- 471 • The reduction in the BSCO, BSHC emissions and smoke opacity by about 10.5%,
472 32%, and 17.4% respectively, is obtained at the higher compression ratio of 18.5,
473 compared to that in case of the original compression ratio.
- 474 • The brake specific nitric oxide emission is greater by about 20% at the compression
475 ratio of 18.5 compared to that of the original operating condition.

476
477 The above experimental findings suggest that the combustion, performance and emission
478 characteristics for the JMEPTO20 blend are relatively better at the higher compression ratio
479 of 18.5 as compared to those at standard operating conditions. Although there is a small
480 increase in the BSNO emission, it still lies within the acceptable range and is quite
481 comparable with that of diesel.

482
483 **References**

- 484 [1] Sher E. Handbook of air pollution from internal combustion engines: pollutant
485 formation and control. Academic Press; 1998.
- 486
487 [2] Rahman AAA. On the emissions from internal-combustion engines: a review
488 International Journal of Energy Research 1998; 22:483-513.
- 489
490 [3] Atmanlı A, Ileri E, Yuksel B. Experimental investigation of engine performance and
491 exhaust emissions of a diesel engine fueled with diesel–n-butanol–vegetable oil
492 blends. Energy Conversion and Management 2014; 81:312-321.
- 493
494 [4] Gautam A, Agarwal AK. Experimental investigations of comparative performance,
495 emission and combustion characteristics of a cottonseed biodiesel-fueled four-stroke
496 locomotive diesel engine. International Journal of Engine Research 2013; 14(4):354-
497 372.

498

- 499 [5] Srivastava PK and Verma M. Methyl ester of karanja oil as alternative renewable
500 source energy. Fuel 2008; 87:1673-1677.
- 501
502 [6] Balat M, Balat H. A critical review of bio-diesel as a vehicular fuel. Energy
503 Conversion and Management 2008; 49:2727-41.
- 504
505 [7] Dixit S, Rehman A. Linseed oil as a potential resource for bio-diesel: a review.
506 Renewable and Sustainable Energy Reviews 2012; 16:4415-4421.
- 507
508 [8] Labeckas G, Slavinskas S. The effect of rapeseed oil methyl ester on direct injection
509 diesel engine performance and exhaust emissions. Energy Conversion and
510 Management 2006; 47:1954-1967.
- 511
512 [9] Kannan D, Pachamuthu S, Nurun NM, Hustad JE, Lovas T. Theoretical and
513 experimental investigation of diesel engine performance, combustion and emissions
514 analysis fuelled with the blends of ethanol, diesel and Jatropha methyl ester. Energy
515 Conversion and Management 2012; 53:322-31.
- 516
517
518 [10] Selim M Y. Reducing the viscosity of Jojoba Methyl Ester diesel fuel and effects on
519 diesel engine performance and roughness. Energy Conversion and Management
520 2009; 50:1781-1788.
- 521
522 [11] Murugan S, Ramaswamy MC, Nagarajan G. Production of tyre pyrolysis oil from
523 waste automobile tyres. Proceedings of National Conference on Advances in
524 Mechanical Engineering 2006; 899-906.
- 525
526 [12] Sharma A, Murugan S. Investigation on the behaviour of a DI diesel engine fueled
527 with Jatropha methyl ester and tyre pyrolysis oil blends. Fuel 2013; 108:699-708.

- 528
529 [13] Kegl B. Effects of biodiesel on emissions of a bus diesel engine. *Bioresource*
530 *Technology* 2008; 99:863-873.
- 531
532 [14] Alla GH, Soliman HA, Badr OH, Rabbo MF. Effect of injection timing on the
533 performance of diesel engine. *Energy Conversion and Management* 2002; 43:269-77.
- 534
535 [15] Papagiannakis RG, Hountalas DT, Rakopoulos CD. Theoretical study of the effects
536 of pilot fuel quantity and its injection timing on the performance and emissions of a
537 dual fuel diesel engine. *Energy Conversion and Management* 2007; 48:2951-2961.
- 538
539 [16] Kegl B. 2006. Experimental investigation of optimal timing of the diesel engine
540 injection pump by using biodiesel fuel. *Energy & Fuels* 2006; 20(4):1460-1470.
- 541
542 [17] Jaichandar S, Senthil Kumar P, Annamalai K. Combined effect of injection timing
543 and combustion chamber geometry on the performance of a biodiesel fueled diesel
544 engine. *Energy* 2012; 47:388-394.
- 545
546 [18] Jaichandar S, Annamalai K. Combined impact of injection pressure and combustion
547 chamber geometry on the performance of a biodiesel fueled diesel engine. *Energy*
548 2013; 55:330-339.
- 549
550 [19] Kannan GR, Anand R. Effect of injection pressure and injection timing on DI diesel
551 engine fuelled with biodiesel from waste cooking oil. *Biomass and Bioenergy* 2012;
552 46:343-352.
- 553
554 [20] Jindal S. Experimental investigation of the effect of compression ratio and injection
555 pressure in a direct injection diesel engine running on Karanj methyl ester.
556 *International Journal of Sustainable Energy* 2011; 30:91-105.

- 557
558 [21] Ye P, Prabhakar B, Boehman A. Experimental investigation of the impact of post-
559 injection on emissions, combustion and lubricant dilution in a diesel engine with B20
560 fuel. *International Journal of Engine Research* 2012; 14(1) 12–22.
- 561
562 [22] Bhusnoor SS, Babu MKG, Subrahmanyam JP. Studies on performance and exhaust
563 emissions of a CI engine operating on diesel and diesel biodiesel blends at different
564 injection pressures and injection timings. *SAE Technical Paper* 2007-01-0613, 2005.
565 Doi: 10.4271/2007-01-0613.
- 566
567 [23] Jindal S, Nandwana BP, Rathore NS, Vashistha V. Experimental investigation of the
568 effect of compression ratio and injection pressure in a direct injection diesel engine
569 running on *Jatropha methyl ester*. *Applied Thermal Engineering* 2010; 30:442-448.
- 570
571 [24] Debnath BK, Sahoo N, Saha UK. Thermodynamic analysis of a variable
572 compression ratio diesel engine running with palm oil methyl ester. *Energy*
573 *Conversion and Management* 2013; 65:147-154.
- 574
575 [25] Muralidharan K, Vasudevan D and Sheeba KN. Performance, emission and
576 combustion characteristics of biodiesel fuelled variable compression ratio engine.
577 *Energy* 2011; 36:5385-5393.
- 578
579 [26] Sharma A, Murugan S. Combustion, performance and emission characteristics of a
580 DI diesel engine fueled with non-petroleum fuel: A study on the role of fuel injection
581 timing. *Journal of the Energy Institute* 2014; article in press.
582 doi:10.1016/j.joei.2014.11.006.

- 583 [27] Sharma A, Murugan S. Impact of fuel injection pressure on performance and
584 emission characteristics of a diesel engine fueled with jatropha methyl ester tyre
585 pyrolysis blend. SAE Technical Paper; 2014-01-2650.
- 586
587 [28] Devan PK, Mahalakshmi NV. A study of performance, emission and combustion
588 characteristics of a compression ignition engine using methyl ester of paradise oil-
589 eucalyptus oil blends. Applied energy 2009; 86:675-680.
- 590
591 [29] Nagaraja S, Sakthivel M, Sudhakaran R. Comparative study of the combustion,
592 performance and emission characteristics of a variable compression ratio engine
593 fuelled with diesel, corn oil methyl ester and palm oil methyl ester. Journal of
594 Renewable and Sustainable Energy 2012; 4:063122.
- 595
596 [30] Cowart JS, Fischer WP, Hamilton LJ, Caton PA, Sarathy SM, Pitz WJ. An
597 experimental and modeling study investigating the ignition delay in a military diesel
598 engine running hexadecane (cetane) fuel. International Journal of Engine Research
599 2012; 14(1) 57–67.
- 600
601 [31] Caton PA, Hamilton LJ and Cowart JS. Understanding ignition delay effects with
602 pure component fuels in a single cylinder diesel engine. ASME Journal of Gas
603 Turbines Power 2011; 133(3).
- 604
605 [32] Gumus MA. Comprehensive experimental investigation of combustion and heat
606 release characteristics of a biodiesel (hazelnut kernel oil methyl ester) fueled direct
607 injection compression ignition engine. Fuel 2010; 89:2802-2814.
- 608
609 [33] Ganesan V, Internal combustion engines. 3rd ed., New Delhi: Tata McGraw-Hill;
610 2010.

- 611 [34] Heywood JB. Internal combustion engine fundamentals. 2nd ed. New York:
612 McGraw-Hill; 1988.
- 613 [35] Muralidharan K, Vasudevan D. Performance, emission and combustion
614 characteristics of a variable compression ratio engine using methyl esters of waste
615 cooking oil and diesel blends. Applied Energy 2011; 88:3959-3968.
- 616
- 617 [36] Martyr A.J., Plint M.A., Engine testing theory and practice. 3rd ed., Oxford:
618 Elsevier; 2007, pp.306-307.
- 619
- 620 [37] Ibrahim A, Adawy ME L, Kassaby MM EL. The Impact of changing the
621 compression ratio on the performance of an engine fueled by biodiesel blends. Energy
622 Technology 2013; 1:395-404.
- 623
- 624 [38] Pundir BP. IC engines, combustion and emissions. Oxford: Alpha Science
625 International Ltd; 2010, pp.-135.
- 626
- 627 [39] Mozhi S VA, Anand RB, and Udayakumar M. Combustion characteristics of
628 diesohol using biodiesel as an additive in a direct injection compression ignition
629 engine under various compression ratios. Energy & Fuels 2009; 23:5413-5422.
- 630
- 631 [40] Jaichandar S and Annamalai K. Effects of open combustion chamber geometries on
632 the performance of pongamia biodiesel in a DI diesel engine. Fuel 2012; 98:272-279.
- 633
- 634 [41] Mani M, Subash C, Nagarajan G. Performance, Emission and Combustion
635 characteristics of a DI diesel Engine using waste plastic oil. Applied Thermal
636 Engineering 2009; 29:2738–2744.
- 637
- 638

- 639 [42] Sharma A, Dhakal B. Performance and Emission Studies of a Diesel Engine Using
640 Biodiesel Tyre Pyrolysis Oil Blends. SAE Technical Paper; 2013-01-1150.
- 641
642 [43] Agrawal AK. Biofuels (alcohols and biodiesel) Applications as Fuels for Internal
643 Combustion Engines. Energy and Combustion Science 2007; 33:233-271.
- 644
645 [44] Kassaby MEL, Nemitallah MA. Studying the effect of compression ratio on an
646 engine fueled with waste oil produced biodiesel/diesel fuel. Alexandria Engineering
647 Journal 2013; 52:1-13.
- 648
649 [45] Pundir BP. Engine emissions: pollutant formation and advances in the control
650 technology. New Delhi: Narosa Publishing House; 2007, pp. - 24.
- 651
652 [46] Sayin C, Canakci M. Effects of injection timing on the engine performance and
653 exhaust emissions of a dual-fuel diesel engine. Energy Conversion and Management
654 2009; 50:203-213.
- 655
656 [47] Agrawal AK, Srivastava DK, Dhar A, Maurya RK, Shukla PC, Singh AP. Effect of
657 fuel injection timing and pressure on combustion, emissions and performance
658 characteristics of a single cylinder diesel engine. Fuel 2013; 111:374-383.
- 659
660 [48] Pundir BP. Engine emissions: pollutant formation and advances in the control
661 technology. New Delhi: Narosa Publishing House; 2007, pp.-51.